



Cosmic radiative feedback from reionization

R. Salvaterra¹, C. Burigana^{2,3}, R. Schneider⁴, T.R. Choudhury⁵,
A. Ferrara⁶, and L. A. Popa^{7,2}

¹ INAF, Osservatorio Astronomico di Brera, via E. Bianchi 46, I-23807 Merate (LC), Italy
e-mail: salvaterra@mib.infn.it

² INAF-IASF Bologna, Istituto di Astrofisica Spaziale e Fisica Cosmica di Bologna, Istituto Nazionale di Astrofisica, via Gobetti 101, I-40129 Bologna, Italy

³ Dipartimento di Fisica, Università di Ferrara, via Saragat 1, I-44100 Ferrara, Italy

⁴ INAF - Osservatorio Astrofisico di Arcetri, Largo Enrico Fermi 5, I-50125 Firenze, Italy

⁵ Institute of Astronomy, Madingley Road, Cambridge CB3 0HA, UK

⁶ SISSA/International School for Advanced Studies, Via Beirut 4, I-34100 Trieste, Italy

⁷ Institute for Space Sciences, Bucharest-Magurele, Str. Atomostilor, 409, PoBox Mg-23, Ro-077125, Romania

Abstract. We explore the effect of cosmic radiative feedback from the sources of reionization on the thermal evolution of the intergalactic medium. We find that different prescriptions for this feedback predict quite different thermal and reionization histories. In spite of this, current data can not discriminate among different reionization scenarios. We find that future observations both from 21-cm and CMB experiments can be used to break the degeneracy among model parameters provided that we will be able to remove the foreground signal at the percent (or better) level.

Key words. Cosmology: theory – galaxies: formation, intergalactic medium

1. Introduction

It is well known that the temperature increase of the cosmic gas in ionized regions leads to a dramatic suppression of the formation of low-mass galaxies (Ciardi & Ferrara 2005). We explore the impact of this effect during cosmic reionization by considering two different feedback prescriptions: (i) *suppression model* where galaxies can form stars unimpeded provided that their circular velocity is larger than a critical threshold, which is not fixed to a constant value but evolves according to gas temperature (Choudhury & Ferrara

2006); (ii) *filtering model*, where, depending on the mass of the galaxy, the fraction of gas available to star formation is reduced with respect of the universal value and it is fully specified by the filtering mass at that redshift (Gnedin 2000).

We implement these two different radiative feedback prescriptions into a physically-motivated and observationally tested model of reionization (Choudhury & Ferrara 2005, 2006). Although the two feedback prescriptions predicts quite different reionization and thermal histories (see Fig. 1), in both scenarios it is possible to reproduce a wide range of observational data with a proper choice of

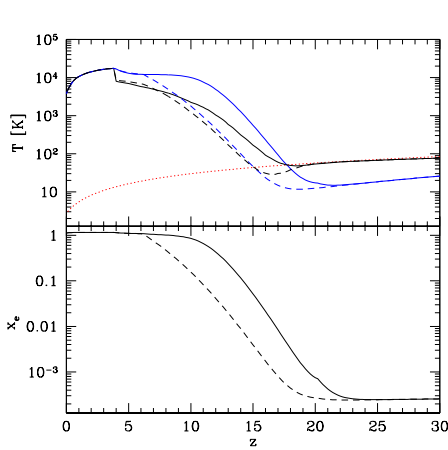


Fig. 1. *Top panel:* redshift evolution of the spin (thick lines) and gas kinetic (thin lines) temperatures predicted by the two models. Solid (dashed) lines refer to suppression (filtering) model. For comparison, we also show the evolution of the CMB temperature T_γ (dotted line). *Bottom panel:* corresponding evolution of the free electron fraction.

few model parameters (the redshift evolution of Lyman-limit absorption systems, the Gunn-Peterson and electron scattering optical depths, the cosmic star formation history, and number counts in high- z sources). Thus, we find that existing data are unable to discriminate among the two reionization histories (Schneider et al. 2008). We then explore alternative methods to break these degeneracies using future 21-cm experiment (Schneider et al. 2008) and CMB anisotropy observations (Burigana et al. 2008).

2. 21-cm signal

The spin temperature T_S , which represents the excitation temperature of the 21 cm transition, determines whether the signal will appear in emission (if $T_S > T_\gamma$) or in absorption (if $T_S < T_\gamma$). Given the different gas ionization fraction and spin temperature evolution in the range $7 \lesssim z \lesssim 20$, the two models predict different global 21 cm background signals in the observed frequency range $75 \text{ MHz} \lesssim \nu \lesssim 200 \text{ MHz}$. The largest differ-

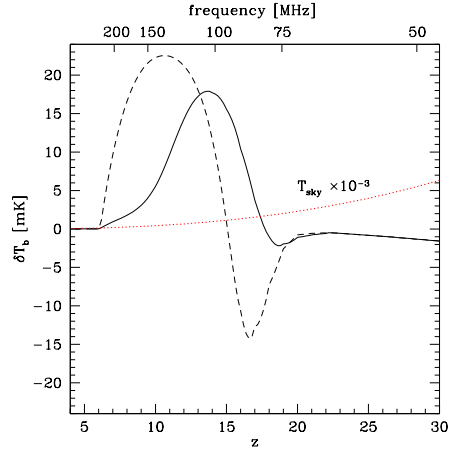


Fig. 2. Predicted all-sky 21 cm brightness temperature relative to the CMB. Solid (dashed) line refers to suppression (filtering) model. The upper x-axis shows a reference observational frequency scale. The dotted line shows an estimate of the foreground signal at these frequencies, rescaled by a factor 10^{-3} .

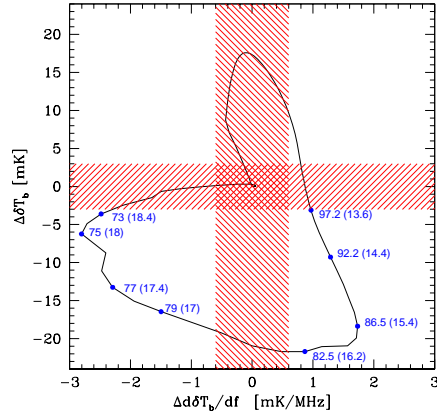


Fig. 3. Difference (filtering – suppression) in the brightness temperature and gradients between the two models (see text). The shaded areas represent the regions where the signals will not be distinguishable given the foreseen sensitivity of future 21 cm experiments. Numbers along the curves indicate the frequency in MHz (and the corresponding redshift) at which the signals would be observed.

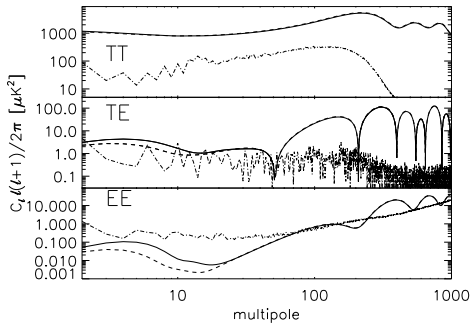


Fig. 4. APS of CMB anisotropies for the three considered modes TT, TE, EE, reported in each panel (solid lines: suppression model; dashes: filtering model). Thick lines denote correlation, while thin lines denote anticorrelation (appearing for the TE mode at $\ell \gtrsim 50$). The APS of the foreground, dominated by the Galactic contribution, is reported for comparison (dot-dashes). Results are expressed in terms of thermodynamic temperature fluctuations.

ences in the two models are represented by a ~ 15 mK absorption feature in the range 75-100 MHz in filtering model (which is nearly absent in suppression model), and by a global shift of the emission feature preceding reionization towards larger frequencies in the same model, as shown in Fig. 2 (Schneider et al. 2008). Since the frequency dependence of the signals and foregrounds are different, the gradient of the brightness fluctuation with frequency might help to discriminate the signal from the relatively smooth foreground in the comparison between the two models, as shown in Fig. 3. Single dish observations with existing or forthcoming low-frequency radio telescopes such as LOFAR, 21CMA, MWA, and SKA can achieve mK sensitivity allowing the identification of these signals provided that foregrounds, which are expected to be three orders of magnitude larger, can be accurately subtracted. The best observational frequencies to discriminate the radiative feedback models through their 21 cm background signal are 73-79 MHz and 82.5-97.2 MHz, where the expected differences in brightness temperatures and gradients are large enough to be detectable with future 21 cm experiments.

3. CMB anisotropies

In this section, we discuss how to discriminate between the two radiative feedback prescriptions (and corresponding reionization histories) with future CMB data (Burigana et al. 2008).

By exploiting the ionization and kinetic temperature histories shown in Fig. 1 we compute the Comptonization and the free-free¹ distortion parameters. We find $u \approx 1.69 \times 10^{-7}$, $y_B \approx 9.01 \times 10^{-10}$ and $u \approx 9.65 \times 10^{-8}$, $y_B \approx 5.24 \times 10^{-10}$ respectively for the suppression and the filtering model. These values are clearly well below the COBE/FIRAS limits. The two models show similar ionization and thermal histories at $z \lesssim 6$ while important differences are predicted at $z \gtrsim 6$, thus explaining the different spectral distortion levels generated in the two cases. The expected Comptonization distortions are comparable to those could be observed in principle by a future generation of CMB spectrum experiments.

We then compute the angular power spectrum (APS) of CMB anisotropy including the ionization history in a dedicated Boltzmann code. Our results are reported in Fig. 4. Having neglected for simplicity tensor perturbations, we focus here on the TT (total intensity, i.e. temperature), TE (temperature-polarization cross-correlation), and EE polarization modes of the CMB anisotropy APS. We also display the APS of the foreground in the V band (centered at 61 GHz) of WMAP 3yr data², a frequency where the foreground is found to be minimum (or almost minimum) in both temperature and polarization at angular scales larger than $\sim 1^\circ$ of relevance in this context.

Fig. 5 shows the relative difference between the EE mode APS of CMB anisotropies, for the suppression and filtering models reported in Fig. 4, compared with the cosmic

¹ The values found for y_B should be considered as lower limits, since they have been computed in the diffuse “averaged density” approximation. Therefore, a correction factor $\approx \langle n^2 \rangle / \langle n \rangle^2 > 1$, coming from a proper inclusion of the treatment of density contrast in the intergalactic medium, should be applied.

² <http://lambda.gsfc.nasa.gov/product/map/current/>

and sampling variance limitation corresponding to a sky coverage of ≈ 74 per cent (region between the dotted lines). We report also for comparison the APS from a potential residual foreground (dot-dashes) corresponding to different values of the relative accuracy (at APS level) of the component separation method in the considered range of multipoles: 0.1 (dashed line), 0.03 (dots-dashed line), 0.01 (three dots-dashed line), and 0.003 (long dashes). The difference between the two considered models is significantly larger than the cosmic and sampling variance over a interesting range of multipoles ($\ell \sim 5 - 15$). The main limitation derives from a possible residual foreground contamination. As evident, a foreground removal accuracy at per cent level (or better) in terms of APS, is necessary to accurately exploit the information contained in CMB polarization about the cosmological reionization process. This calls for a further progress in component separation techniques in polarization and for an accurate mapping of the (mainly Galactic) polarized foregrounds in radio and far-IR bands to complement microwave surveys by improving both the foreground physical modeling and the component separation accuracy.

While the difference between the APS of CMB anisotropies in the two models is overwhelmed by (respec. not significantly larger than) the cosmic and sampling variance for the TT (respec. the TE) mode, we find that future accurate large sky coverage observations of EE polarization mode (e.g. from the forthcoming ESA *Planck* mission³ or from the next generation of polarization dedicated satellites, as CMBPol and B-Pol⁴) can be used to discriminate between the two reionization histories.

4. Conclusions

We have explored the effect of cosmic radiative feedback from the sources of reionization on the thermal evolution of the intergalactic medium. We implemented two different prescriptions for this feedback into a well-tested, physically-motivated model of the early

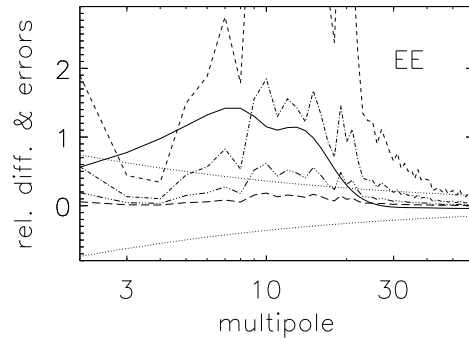


Fig. 5. Relative difference between the (EE mode) APS of CMB anisotropies for the suppression and filtering models (thick solid lines) is compared with the cosmic and sampling variance limitation (dotted lines) and different foreground residual (dot-dashed lines). See the text for more details.

Universe. We found that different prescriptions for this feedback predict quite different thermal and reionization histories. In spite of this differences, current data can not discriminate among different reionization scenarios. Therefore, we explored alternative methods to break this degeneracies using 21-cm experiment and CMB anisotropy observations. We found that future data can distinguish among different reionization histories provided that we would be able to remove the foreground signal at the percent (or better) level.

References

- Burigana C., Popa L.A., Salvaterra R., Schneider R., Choudhury T.R., Ferrara A., 2008, MNRAS, 385, 404
- Choudhury T.R. & Ferrara A., 2005 MNRAS, 361, 577
- Choudhury T.R. & Ferrara A., 2006, MNRAS, 371, L55
- Ciardi B. & Ferrara A., 2005, Space Sci. Rev., 116, 625
- Gnedin N., 2000, ApJ, 542, 535
- Schneider R., Salvaterra R., Choudhury T.R., Ferrara A., Burigana C., Popa L.A., 2008, MNRAS, 384, 1525

³ <http://www.rssd.esa.int/planck>

⁴ <http://www.th.u-psud.fr/bpol/index.php>